7. Optimization of Coiled Coil Based Amyloids

To practically realize the design ideas presented in section 6.3, an evolutional design strategy has been applied. Prior to the incorporation of structural switches, an appropriate coiled coil based model peptide system that slowly converts into amyloids had to be developed as the leading sequence for further modifications. This development procedure is described in the following section.

7.1 Ideal α-Helical Coiled Coils

7.1.1 VW01

In the first step, an ideally folded 26 residue coiled coil peptide termed VW01 has been designed and characterized. Figure 7.1 shows the helical wheel diagram (from N- to C-terminus) and the sequence of peptide VW01.

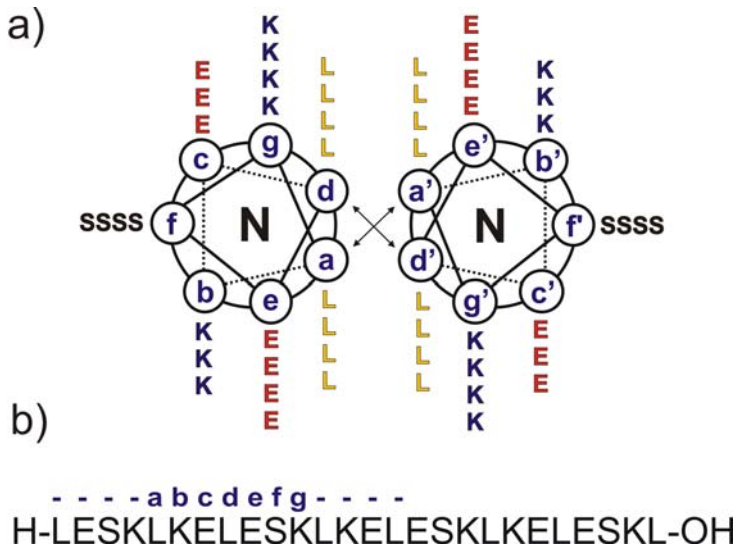

Figure 7.1. *(a) Helical wheel diagram and (b) sequence of the idealized coiled coil peptide VW01.*

The design is optimized for perfect parallel coiled coil folding. Positions a and d within the *heptad* repeat are exclusively occupied by hydrophobic leucine residues, which ensures an efficiently packed hydrophobic core (first recognition domain). Furthermore,

positions e and g are exclusively equipped with charged glutamic acid and lysine residues, respectively, forming attractive Coulomb interactions in case of a parallel helix alignment (second recognition motif). The adjacent b and c positions are occupied by oppositely charged lysine or glutamate residues which further stabilize the α-helical structure by intramolecular ion-pairing.

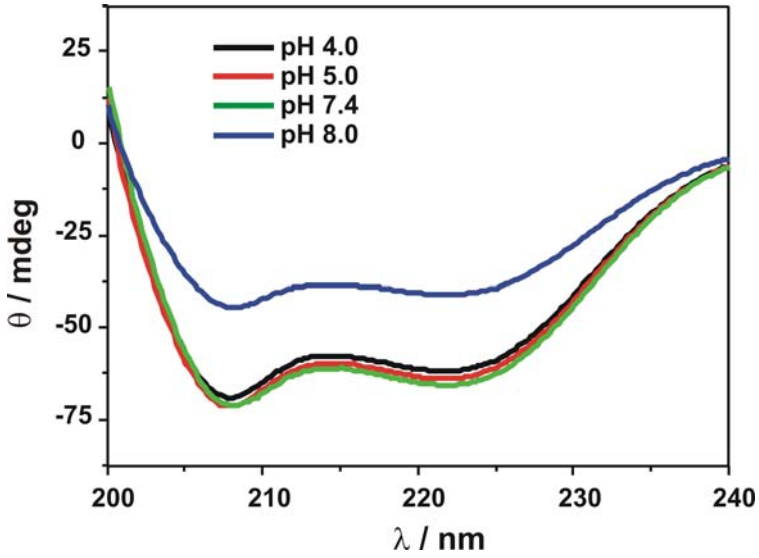

Figure 7.2. *CD spectra of peptide VW01 at different pH values (c ~ 250μM, 10mM buffer, pH 4.0 - 5.0: acetate buffer, pH 7.4 – 8.0: Tris/HCl buffer).*

Figure 7.2 shows the obtained CD spectra at a peptide concentration of approx. 250μM. Similar spectra have been obtained for lower concentrations (data not shown). As expected, peptide VW01 adopts an α-helical conformation in the complete pH-range from 4.0 to 8.0 as indicated by two characteristic minima at 208 and 222nm. Furthermore, the stability of the helical folding at pH 4.0, 7.4, and 8.0, respectively, was followed by temperature-dependent CD spectroscopy. To observe the unfolding process of α-helices the intensity of the characteristic minima at 222nm was measured at different temperatures and concentrations of denaturizing agent and shows a typical sigmoidal curve shape. During the process of denaturation the CD spectrum is moving from helical (λ_{min} = 208 and 222nm) to random coil (λ_{min} = 200nm). Figure 7.3 exemplarily shows the denaturation profile of VW01 at pH 7.4 and different concentrations of guanidine hydrochloride (GndHCl). Without addition of GndHCl peptide VW01 cannot be unfolded completely by heat as indicated by the black curve. Contrarily, complete denaturation is observed in presence of 3M GndHCl.

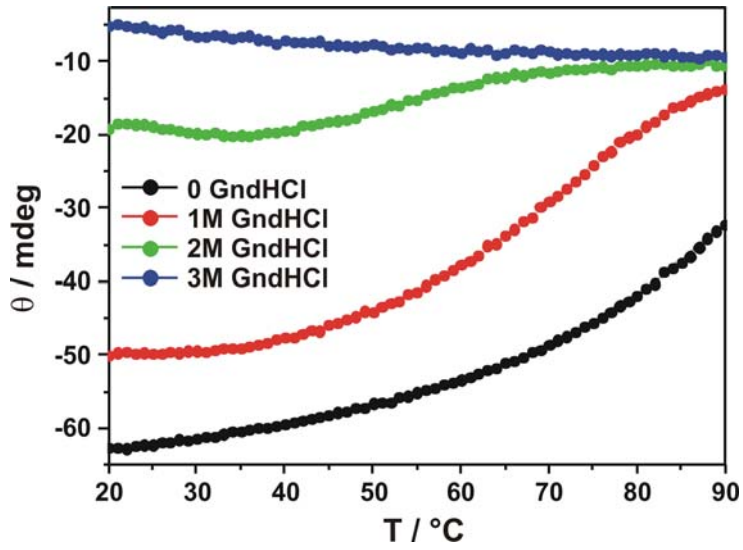

Figure 7.3. *Temperature denaturation profiles of peptide VW01 at pH 7.4. (c ~ 100µM, 10mM Tris/HCl buffer).*

In order to at least partially achieve comparable data from the denaturation profiles, the melting temperatures at which 50% of the peptide unfolds have been determined. These values have been obtained by direct comparison of the ellipticities at the fully folded state (0 GndHCl and 20°C) and the fully unfolded state (3M GndHCl, 90°C). Table 7.1 shows the calculated melting points of peptide VW01 at pH 4.0, 7.4, and 8.0, respectively. As already assumed from the CD spectra, peptide VW01 adopts a stable α-helical coiled coil with comparable stabilities in the observed pH range. Thus, it represents an ideal basis for the development of amyloid forming coiled coil peptides.

Table 7.1. *Melting temperatures of peptide VW01 at different pH values and GndHCl concentrations (c ~ 100µM, 10mM buffer, pH 4.0: acetate buffer, pH 7.4: Tris/HCl buffer, pH 8.0: phosphate buffer).*

pH	Melting temperature in °C at			
	0 GndHCl	1M GndHCl	2M GndHCl	3M GndHCl
4.0	77.7	70.2	53.8	unfolded
7.4	86.2	62.5	>50% unfolded	unfolded
8.0	90.0	73.8	40.5	unfolded

7.1.2 VW02

Subsequently, the permutability of the charged residues within the coiled coil has been investigated. Therefore, the residues at positions e and g as well as at b and c have been exchanged by their complementarily charged counterparts (Lys→Glu, Glu→Lys), yielding peptide VW02. Figure 7.4 shows a helical wheel diagram and the sequence of VW02.

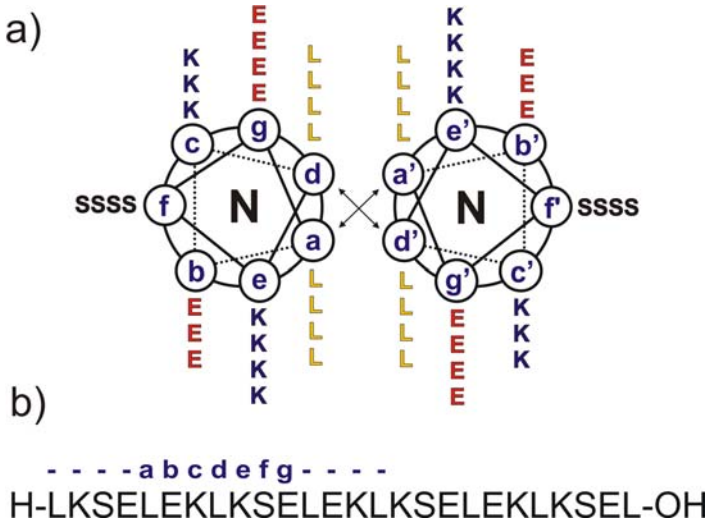

Figure 7.4. *(a) Helical wheel diagram and (b) sequence of the idealized coiled coil peptide VW02.*

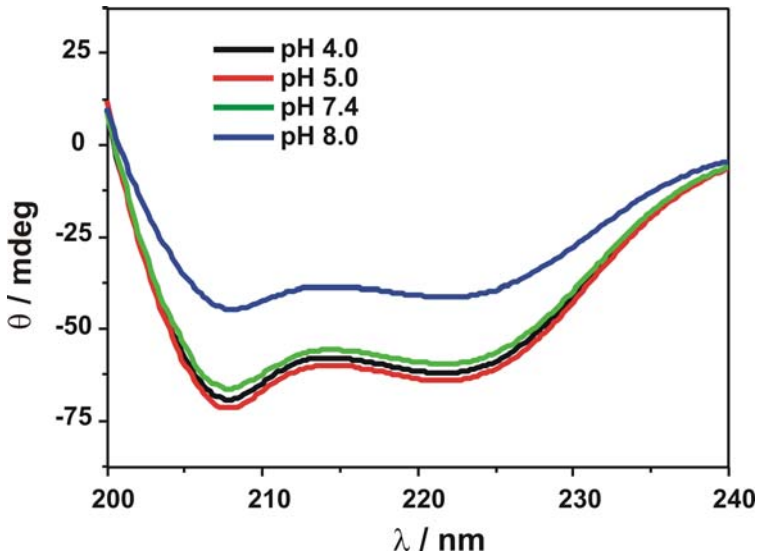

Figure 7.5. *CD spectra of peptide VW02 at different pH values (c ~ 250µM, 10mM buffer, pH 4.0 - 5.0: acetate buffer, pH 7.4 – 8.0: Tris/HCl buffer).*

Not surprisingly, peptide VW02 adopts an α-helical conformation as indicated by the CD spectra which are almost identical to those obtained for peptide VW01 (Figure 7.5). Thus, it can be reasoned that there are no notable distinctions between positions e and g, and b and c, respectively, for this particular parallel coiled coil system.

7.2 The Way from β-Sheet to α-Helix

In the next step, the two previously described, perfectly folded coiled coil peptides have been modified to generate an α-helical peptide with an intrinsic amyloid formation propensity. During the work on this thesis, this issue turned out to be complicated. The absence of well determined cross-strand amino acid preferences in β-sheets and amyloids hampers a balanced fusion of coiled coil and β-sheet design principles. Thus, many peptides with sequences related to each other had to be synthesized until an optimized amyloid forming coiled coil sequence was identified. This bottom-up evolution is described in the following subsections.

7.2.1 VW11

Inspired by the early works of the groups of Mutter[131,132] and Gellman,[133] the ideally folded 26 residue coiled coil peptide was vigorously modified by incorporating features which enable the formation of an amphiphilic β-sheet structure. Figure 7.6 shows the first designed β-sheet peptide VW11 as helical wheel model and as an extended parallel β-sheet aligned in a zigzag fashion. As the most important design feature, five hydrophobic and β-sheet preferring valine residues have been incorporated at the b, c, and f positions of the coiled coil *heptad* repeat. In case of an extended β-sheet structure, a highly hydrophobic interface containing exclusively leucine, valine and serine residues would form, while the other face of the sheet would be mainly occupied by charged residues. Thus, this peptide is expected to exhibit a strong preference for an amphiphilic β-sheet structure. Nevertheless, the leucine residues at positions a and d which form the coiled coil's hydrophobic core have been kept unchanged in order to maintain a certain helix forming propensity. In contrast, positions e and g are occupied by alternating Glu and Ser residues. Thus, only repulsive intermolecular Coulomb interactions would occur in case of a helical folding. Therefore, this peptide in summary exhibits a strong preponderance of features that promote the formation of β-sheets and amyloids.

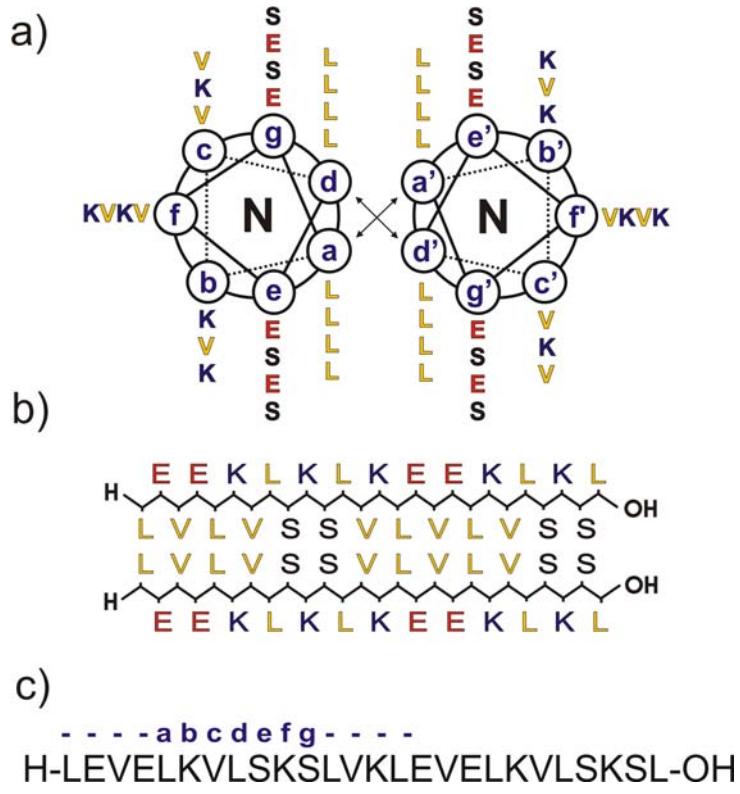

Figure 7.6. *(a) Helical wheel diagram, (b) zigzag model of a parallel β-sheet, and (c) sequence of the basic β-sheet peptide VW11.*

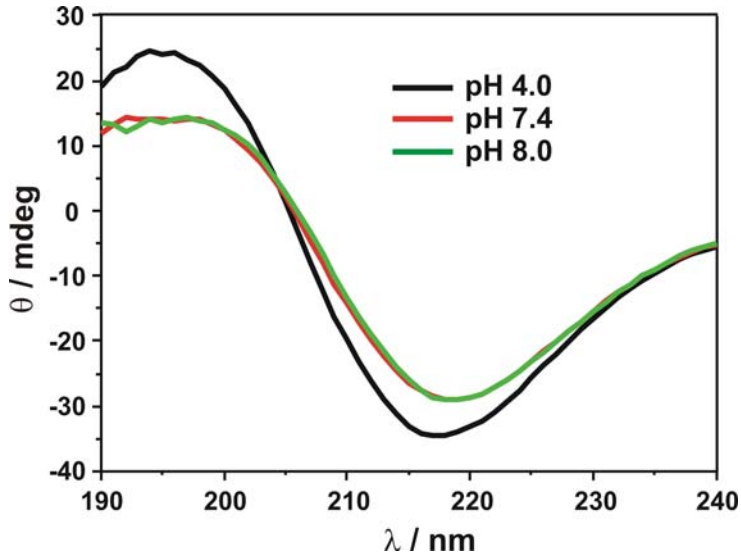

Figure 7.7. *CD spectra of peptide VW11 at different pH values (c ~ 200µM, 10mM buffer, pH 4.0: acetate buffer, pH 7.4: Tris/HCl buffer, pH 8.0: phosphate buffer).*

The observed folding behavior shown in Figure 7.7 explicitly confirms the underlying design. Only β-sheet CD signatures with one prominent minimum at 216nm and a maximum at 195 nm have been obtained for a peptide concentration of approximately 100µM and a pH ranging from 4.0 to 8.0. Similar spectra have been measured for lower concentrations up to approx. 25µM (data not shown). Thus, peptide VW11 doubtlessly forms amphiphilic β-sheets in a wide range of concentrations and pH values. Based on the primary structure of VW11, the following peptides have been successively modified with features that increase the coiled coil formation propensity again until a balanced level was reached.

7.2.2 VW12

Peptide VW12 represents the first evolutional step of the basic β-sheet forming sequence VW11 on the way to an amyloid forming coiled coil. Figure 7.8 shows the modified sequence as helical wheel model and as an extended parallel β-sheet aligned in a zigzag fashion.

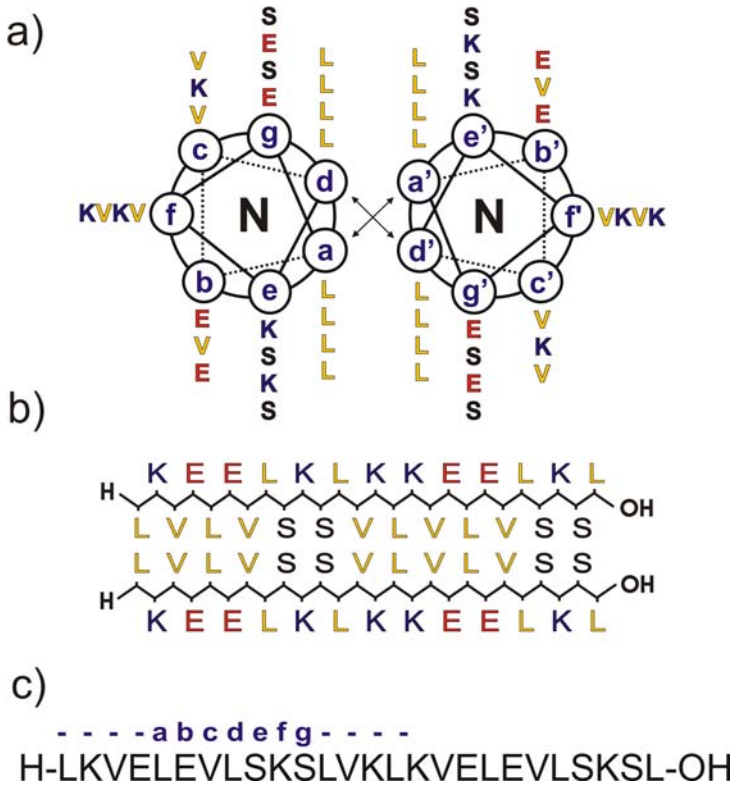

Figure 7.8. *(a) Helical wheel diagram, (b) zigzag model of a parallel β-sheet, and (c) sequence of peptide VW12.*

In order to slightly increase the propensity of a helical folding, the charged Glu and Lys residues at positions b and e have been replaced by each other, which facilitates attractive intermolecular Coulomb interactions in a helical folding. The remaining positions have been retained to ensure the necessary comparability to peptide VW11.

Figure 7.9 shows the obtained CD spectra at pH 4.0, 7.4, and 8.0 at a peptide concentration of approx. 200µM. Although intermolecular electrostatic interactions between e and g positions are known to facilitate the coiled coil formation, this effect appears to be inconsiderable in peptide VW12. The CD spectra are similar to those obtained for peptide VW11 and clearly indicate the presence of a β-sheet structure. Lower concentrations up to approx. 25µM did not change the conformation significantly (data not shown). Thus, further modification steps were needed to converge to the proposed α-helical coiled coil conformation.

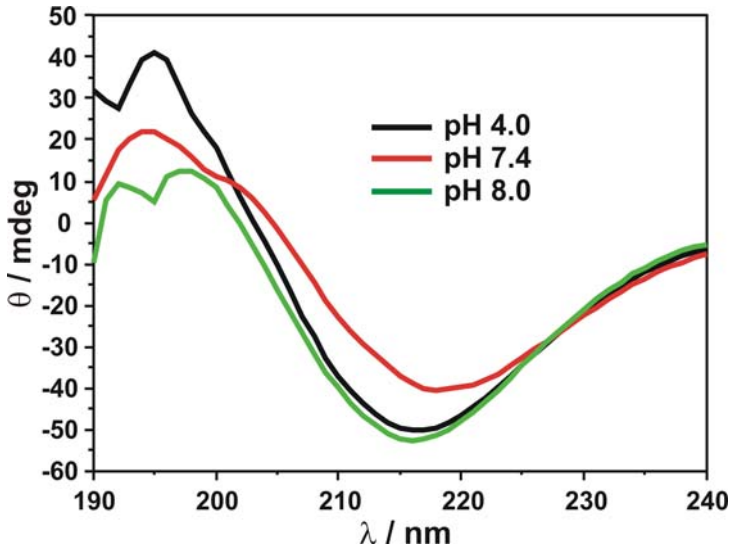

Figure 7.9. *CD spectra of peptide VW12 at different pH values (c ~ 200µM, 10mM buffer, pH 4.0: acetate buffer, pH 7.4: Tris/HCl buffer, pH 8.0: phosphate buffer).*

7.2.3 VW13

Due to the unchangeably high β-sheet formation tendency of peptide VW12, the hydrophobic residues Val in positions b, c, and f of the coiled coil *heptad* repeat attracted further attention. The highly hydrophobic face formed by Leu, Val, and Ser residues is apparently the major thermodynamic driving force for the formation of an amphiphilic β-sheet. Thus, removing one of the Val residues at the solvent exposed coiled coil posi-

tions should predictably decrease the β-sheet formation tendency. Figure 7.10 shows the sequence of the resulting peptide VW13 as helical wheel model and as an extended parallel β-sheet aligned in a zigzag fashion. In comparison to peptide VW12, one Val residue at *heptad* repeat position f was replaced by Ser in order to disrupt the central hydrophobic β-sheet core. The remaining positions have been kept unchanged.

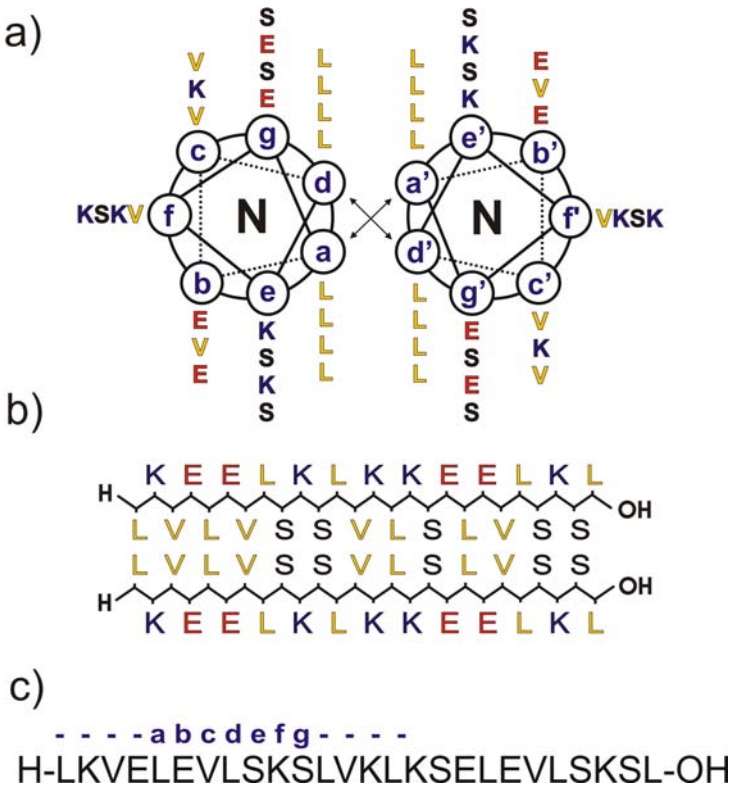

Figure 7.10. *(a) Helical wheel diagram, (b) zigzag model of a parallel β-sheet, and (c) sequence of peptide VW13.*

Figure 7.11 shows the CD spectra at pH 4.0, 7.4, and 8.0 and a peptide concentration of approx. 200µM. The spectra doubtlessly show typical β-sheet signatures similar to those obtained for the previously described peptides VW11 and VW12. Lower concentrations up to approx. 25µM yielded almost analogous spectra (data not shown). Only a slight shoulder around 200nm appeared at pH 4.0 and concentrations below 50µM, pointing to a small fraction of unfolded peptide. However, further steps are needed to decrease the high β-sheet formation tendency of the model system to a controllable level.

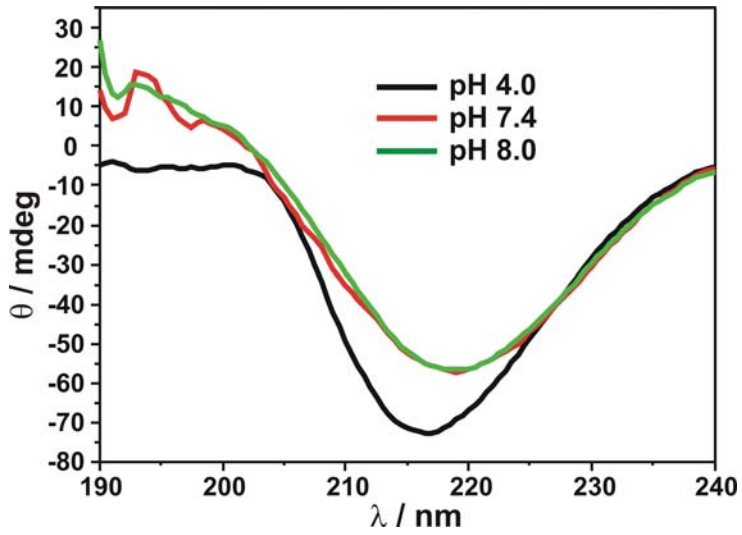

Figure 7.11. *CD spectra of peptide VW13 at different pH values (c ~ 200µM, 10mM buffer, pH 4.0: acetate buffer, pH 7.4: Tris/HCl buffer, pH 8.0: phosphate buffer).*

7.2.4 VW16

The results of peptide VW13 clearly showed that the model system still exhibits an unfeasibly high β-sheet formation tendency. Thus, one more Val residue at the solvent exposed c position was removed in the next evolutional step, yielding peptide VW16. Figure 7.12 shows the sequence of peptide VW16 as helical wheel model and as an extended parallel β-sheet aligned in a zigzag fashion. In contrast to VW13, Valine was not directly replaced by Ser, but exchanged by Lys to gain two simultaneously occurring effects. First, the hydrophobicity at the solvent exposed b, c, and f positions is reduced and, therefore, a lower propensity for β-sheet formation is expected. Additionally, two Lys residues at position c are now placed adjacent to the Glu residues at position g and, thus, facilitate intrahelical salt bridges that should further stabilize the helical structure. Nevertheless, the observed effects on the conformation of VW16 were weaker than expected. Figure 7.13 shows the CD spectra at pH 4.0, 7.4, and 8.0 and a peptide concentration of approx. 200µM.

Peptide VW16 adopts a clear β-sheet conformation in the observed pH range from 4.0 to 8.0. Additionally, the low intensity at pH 7.4 and the high overall absorbance at wavelengths below 200nm points to a rapid peptide aggregation at these comparatively high concentrations of approx. 200µM. Decreasing the concentration at pH 7.4 and 8.0 yielded similar spectra without interfering absorption (data not shown).

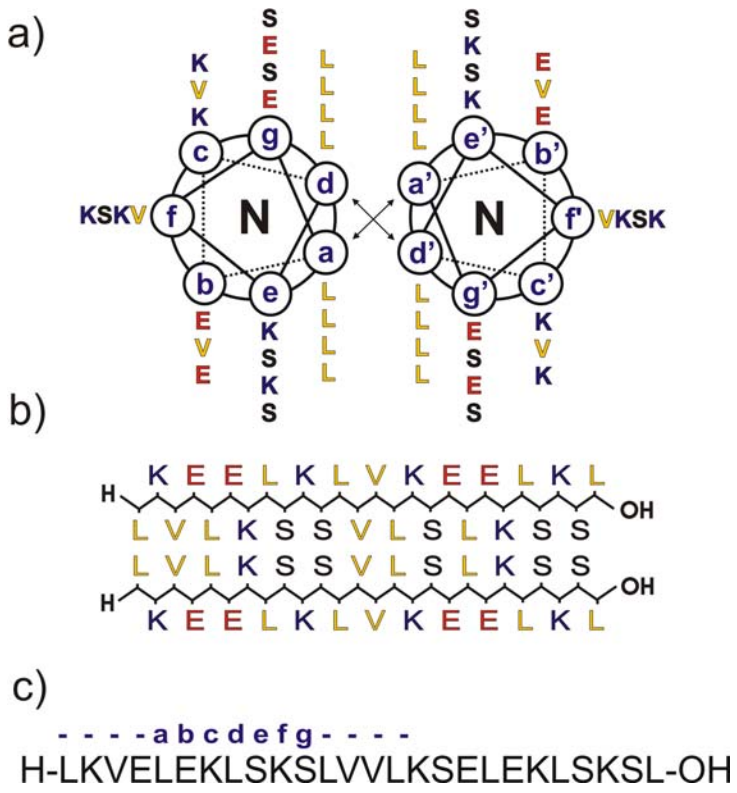

Figure 7.12. *(a) Helical wheel diagram, (b) zigzag model of a parallel β-sheet, and (c) sequence of peptide VW16.*

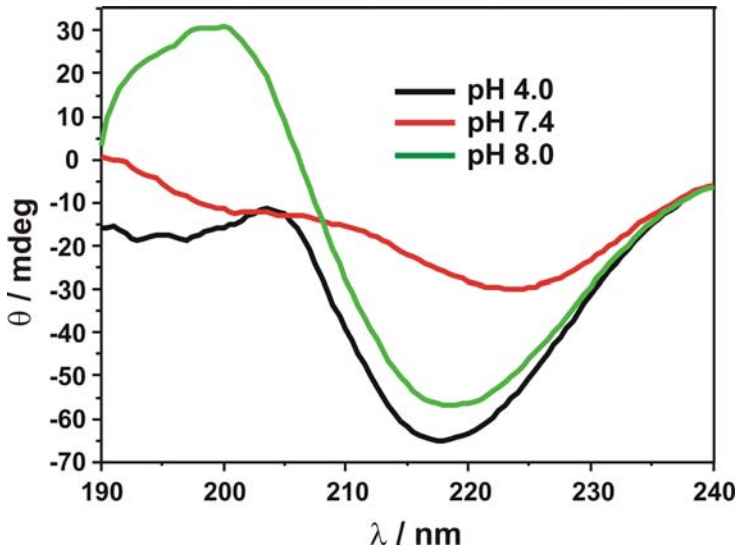

Figure 7.13. *CD spectra of peptide VW16 at different pH values (c ~ 200µM, 10mM buffer, pH 4.0: acetate buffer, pH 7.4: Tris/HCl buffer, pH 8.0: phosphate buffer).*

However, at pH 4.0 and lower concentrations an interesting concentration dependency of the conformation has been observed. Figure 7.14 shows CD spectra of peptide VW16 at pH 4.0 and different concentrations. Successive decrease of the concentration from approx. 100µM to 25µM yields mixed spectra containing a fraction of unfolded peptide in addition to the β-sheet obtained at approx. 200µM. The relative content of random coil increases with decreasing peptide concentration and at approx. 25µM almost complete unfolding is observed. Interestingly, the appearance of a slight shoulder in the spectra of VW13 at pH 4.0 and concentrations below 50µM resembles the behavior of VW16, although the observed effects were less distinct. Apparently, this concentration dependency at acidic pH arises from the slight excess of basic amino acids in both peptides. Peptide VW13 contains five and peptide VW16 six basic Lys residues, while both peptides contain only four acidic Glu residues. At pH 4.0, most of the charged side chains in VW13 and VW16 are protonated, yielding an overall charge of +4 and +5, respectively. As a result, undirected repulsive Coulomb interactions between the protonated Lys residues may act destabilizing on any type of peptide conformation at acidic pH values. During the work on this thesis, similar excessively charged domains have been applied selectively as pH sensitive structural triggers (see section 8.1).

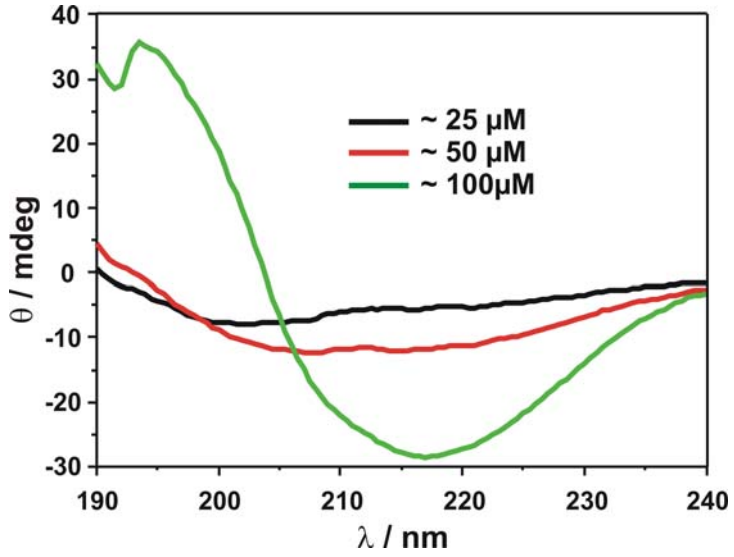

Figure 7.14. *CD spectra of peptide VW16 at pH 4.0 and different concentrations (black: c ~ 25µM, red: c ~ 50µM, and green: c ~ 100µM, 10mM acetate buffer, pH 4.0).*

Although peptide VW16 still exhibits a high tendency to adopt a β-sheet structure, it represents an important landmark for the evolutional design of an amyloid forming coiled coil system. The concentration dependency at pH 4.0 suggests that the balanced level for the incorporation of other structural features beside the high intrinsic β-sheet formation propensity is reached. Thus, the three hydrophobic Val residues at b, c, and f positions of the *heptad* repeat have been maintained in the following peptides.

7.2.5 VW17

Peptide VW17 is a direct descendant of VW16. Figure 7.15 shows the sequence of peptide VW17 as helical wheel model and as an extended parallel and antiparallel β-sheet aligned in a zigzag fashion.

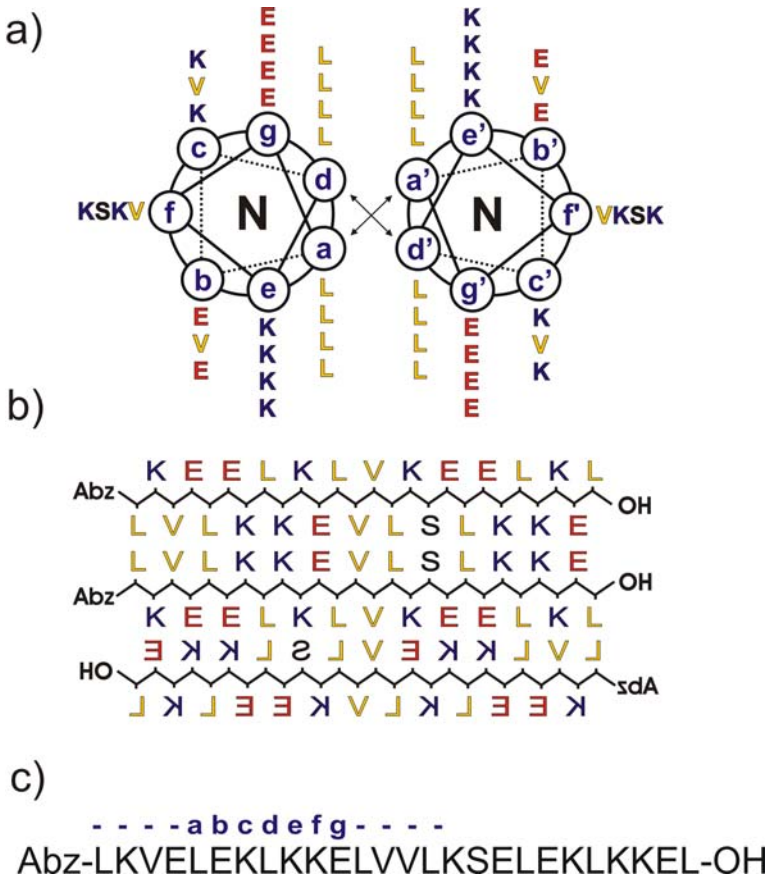

Figure 7.15. *(a) Helical wheel diagram, (b) zigzag model of a parallel and an anti-parallel β-sheet, as well as (c) sequence of peptide VW17.*

In order to increase the peptide's ability to adopt an α-helical coiled coil conformation, Ser residues at position e and g have been exchanged by Lys and Glu, respectively, facilitating attractive interhelical Coulomb interactions between the helices. Additionally, this is accompanied by an increased α-helix propensity, since Lys and Glu exhibit a strong overall preference for α-helical structures, while Ser features no defined structural preferences.[217,220] Furthermore, the highly hydrophobic face in the extended parallel β-sheet is perceptibly disrupted, since the positively and negatively charged residues are now evenly distributed on both sides of the β-strands. As a result, an antiparallel orientation of the β-sheets with complementary pairing of charges has to be considered as possible structure instead (Figure 7.15 b).

Surprisingly, peptide VW17 adopted a clear α-helical conformation directly after dissolution. Figure 7.16 shows the CD spectra of VW17 at pH 4.0, 7.4, and 8.0 and a peptide concentration of 100µM. However, amyloid formation is a time dependent process. Thus the conformation of VW17 was monitored over 72h in order to observe possible structural changes that indicate the time dependent association into amyloids. Interestingly, no structural transitions were observed for the entire pH range from 4.0 to 8.0. Figure 7.17 exemplarily shows CD spectra of peptide VW17 at pH 4.0 recorded after different times of incubation. Similar spectra have been obtained for pH 7.4 as well as 8.0 (data not shown).[221]

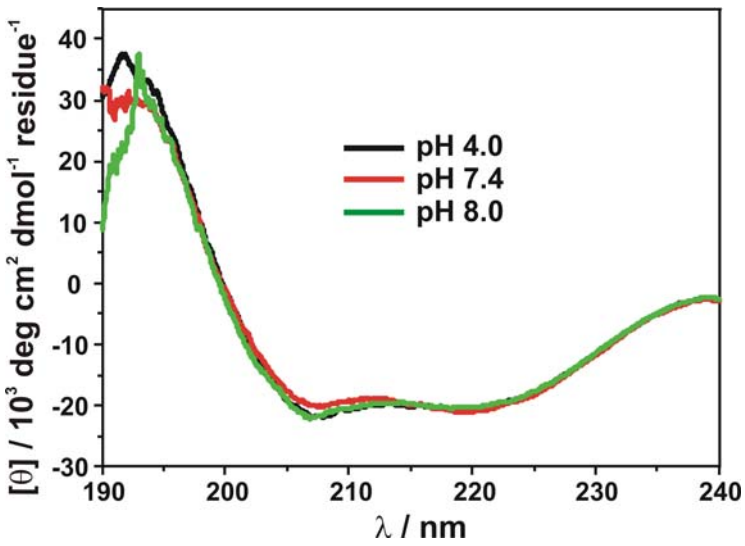

Figure 7.16. *CD spectra of peptide VW17 at different pH values (c = 100µM, 10mM buffer, pH 4.0: acetate buffer, pH 7.4: Tris/HCl buffer, pH 8.0: phosphate buffer).*

These data indicate that VW17 does not form amyloids within a time range of three days. Apparently, the further enhancement of the model's α-helix propensity results in the formation of stable α-helical coiled coils which do not convert into amyloids at ambient conditions. Hence, a further reinforcement of the system's β-sheet formation propensity should yield the intended amyloid formation properties.

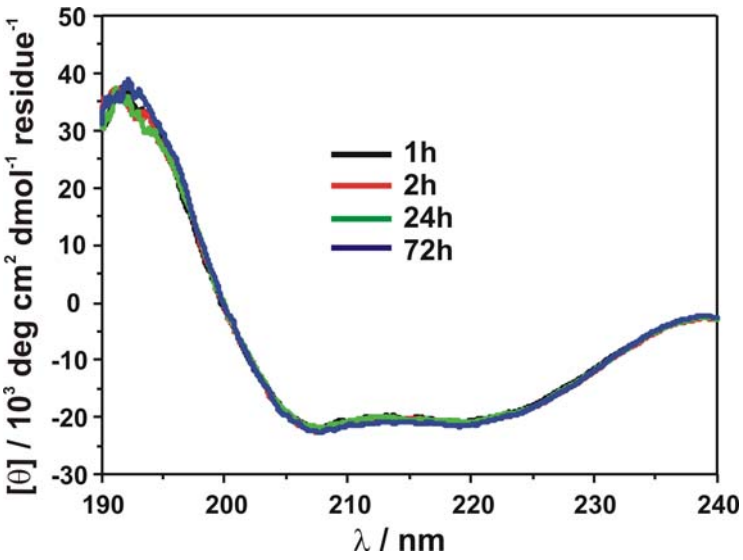

Figure 7.17. *CD spectra of peptide VW17 at pH 4.0 after 1, 2, 24, and 72h (c = 100µM, 10mM acetate buffer, pH 4.0).*

7.2.6 VW18

The results of VW16 and VW17 impressively highlighted the enormous impact of a well balanced interplay between α-helical coiled coil stability and β-sheet formation propensity for the design. In order to indirectly enhance the β-sheet propensity of VW17 without affecting the ability to adopt a helical conformation, the two helix preferring Lys residues at position f were replaced by Ser, which does not possess defined structural preferences. Figure 7.18 shows the sequence of peptide VW18 as helical wheel model and as an extended parallel and antiparallel β-sheet aligned in a zigzag fashion. Seen from a different angle, the design of VW18 completes the circle of the evolutional design approach. In principle, the sequence corresponds to the ideally folded α-helical coiled coils VW01 and VW02 that have been equipped with three Val residues as amyloid inducing feature.

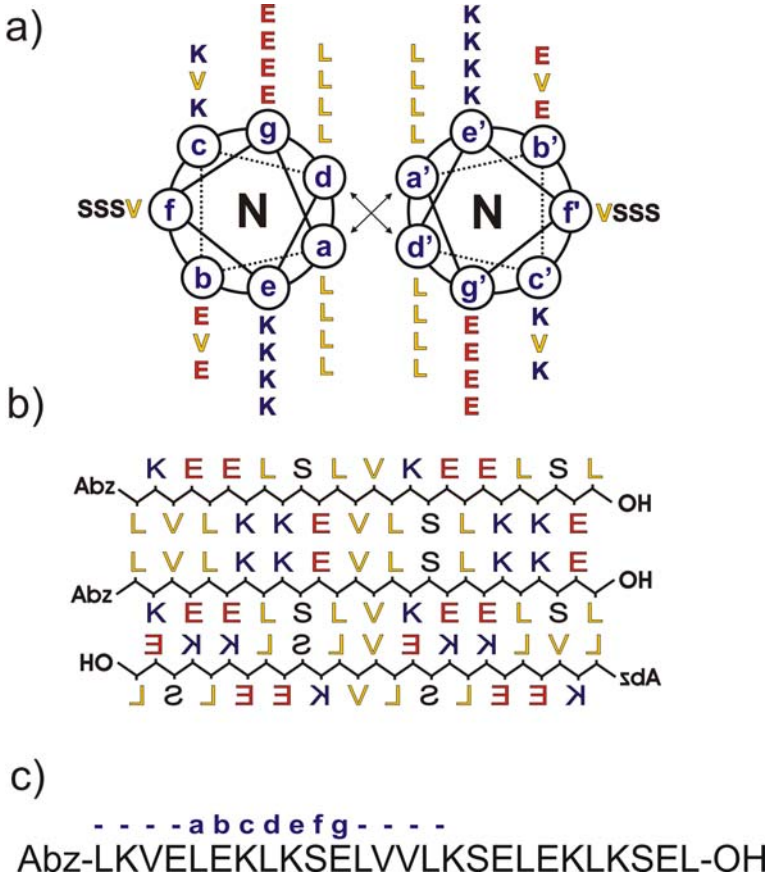

Figure 7.18. *(a) Helical wheel diagram, (b) zigzag model of a parallel and an anti-parallel β-sheet, as well as (c) sequence of the peptide VW18.*

Directly after dissolution, peptide VW18 adopts a clear α-helical conformation for the entire pH range from 4.0 to 8.0. Figure 7.19 shows the CD spectra of VW18 at pH 4.0, 7.4 and 8.0 and a peptide concentration of 100µM. Nevertheless, a time dependent conformational transition to a β-sheet rich conformation is observed at pH 7.4 as well as pH 8.0, suggesting an amyloid formation at these conditions within two to three days. Figure 7.20 exemplarily shows CD spectra of VW18 at pH 7.4 recorded after different incubation times. A similar behavior has been observed for concentrations up to 330µM at pH 7.4 as well as 8.0 (data not shown).[221,222]

Interestingly, at pH 4.0 and a comparable concentration of 100µM the peptide stays α-helical (data not shown).[221,223] Apparently, the stability of the α-helical coiled coil structure at acidic conditions where all charged side chains are protonated is distinctly higher than at neutral or slightly basic pH with a balanced distribution of charges. This is not surprising and similar effects have been reported in the literature. In general, most of the known coiled coil peptides are more stable at acid conditions compared to

neutral pH.[224] Hodges and co-workers found that protonated Glu residues in comparison to ionic Glu stabilize the α-helical coiled coil structure at acid conditions.[224] Especially at e and g positions, protonated Glu residues perceptibly increase the coiled coil stability caused by an enhanced hydrophobicity at positions close to the hydrophobic core.[225,226]

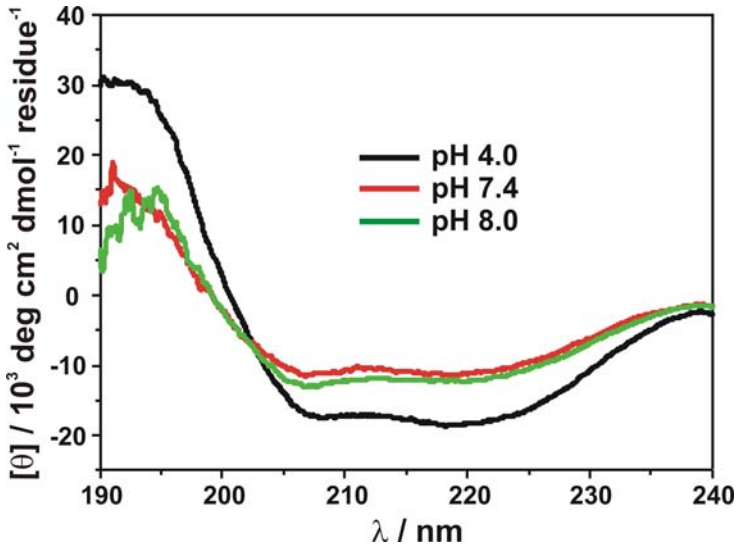

Figure 7.19. *CD spectra of peptide VW18 at different pH values (c = 100µM, 10mM buffer, pH 4.0: acetate buffer, pH 7.4: Tris/HCl buffer, pH 8.0: phosphate buffer).*

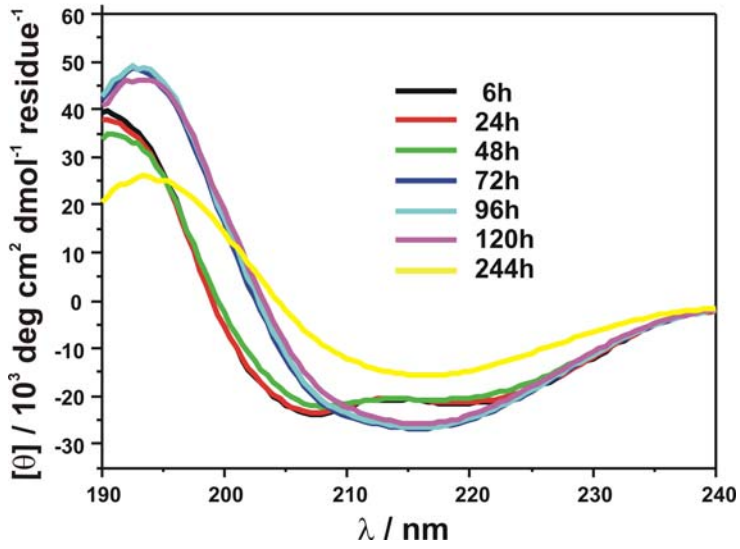

Figure 7.20. *CD spectra of peptide VW18 at pH 7.4 after different incubation times (c = 95µM, 10mM phosphate buffer, pH 7.4).*

However, the occurrence of β-sheet CD signature at pH 7.4 and 8.0 is not sufficient proof for the presence of amyloids. Thus, a diagnostic ThT scan was performed to verify the expected amyloid formation process (Figure 7.21). The time dependent sigmoidal increase of the ThT fluorescence that was observed indicates a typical nucleation dependent amyloid association process (see section 4.2). The measured time course moreover confirms the CD data that suggested a slow amyloid formation within two to three days. Additionally, Congo red binding studies on VW18 (data not shown) further substantiated the presence of amyloids.[223]

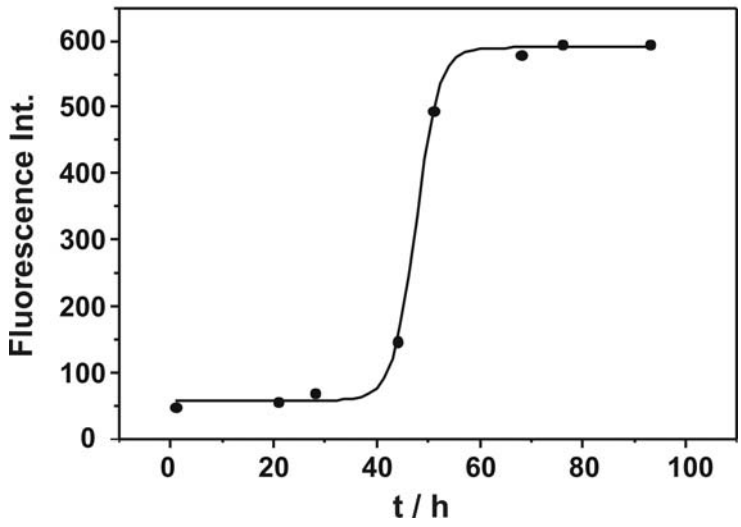

Figure 7.21. *ThT assay of peptide VW18 at pH 7.4 after different incubation times (50µM VW18, 50µM ThT, 10mM phosphate buffer, pH 7.4).*

In conclusion, the evolutional design approach was successfully used to generate a coiled coil based model system that forms amyloids at appropriate conditions without the unnatural stimulus of elevated temperatures. Starting with an α-helical conformation, peptide VW18 doubtlessly associates into amyloids within days at neutral and slightly basic conditions. As a result, peptide VW18 represent a perfect basis for the second step of the design - the incorporation of functionalities that sensitively react to altered environmental conditions.